Violation of entropic Leggett-Garg inequality in nuclear spins

Hemant Katiyar,[1] Abhishek Shukla,[1] K. Rama Koteswara Rao,[2] and T. S. Mahesh[1,*]
[1]*Department of Physics and NMR Research Center, Indian Institute of Science Education and Research, Pune 411008, India*
[2]*Department of Physics and NMR Research Centre, Indian Institute of Science, Bangalore 560012, India*

(Received 8 November 2012; published 2 May 2013)

We report an experimental study of recently formulated entropic Leggett-Garg inequality (ELGI) by Usha Devi *et al*. [Phys. Rev. A **87**, 052103 (2013)]. This inequality places a bound on the statistical measurement outcomes of dynamical observables describing a macrorealistic system. Such a bound is not necessarily obeyed by quantum systems, and therefore provides an important way to distinguish quantumness from classical behavior. Here we study ELGI using a two-qubit nuclear magnetic resonance system. To perform the noninvasive measurements required for the ELGI study, we prepare the system qubit in a maximally mixed state as well as use the "ideal negative result measurement" procedure with the help of an ancilla qubit. The experimental results show a clear violation of ELGI by over four standard deviations. These results agree with the predictions of quantum theory. The violation of ELGI is attributed to the fact that certain joint probabilities are not legitimate in the quantum scenario, in the sense they do not reproduce all the marginal probabilities. Using a three-qubit system, we also demonstrate that three-time joint probabilities do not reproduce certain two-time marginal probabilities.

DOI: 10.1103/PhysRevA.87.052102 PACS number(s): 03.65.Ud, 03.65.Ta, 03.67.Ac, 03.67.Lx

I. INTRODUCTION

The behavior of quantum systems is often incomprehensible by classical notions, the best examples being nonlocality [1,2] and contextuality [3]. Quantum systems are *nonlocal* since they violate Bell's inequality derived from the *locality* assumption, i.e., operations on one of the two spacelike separated objects can not disturb the measurement outcomes of the other [4]. The quantum systems are also *contextual* in the sense that a measurement outcome depends not only on the system and the property being measured, but also on the context of the measurement, i.e., on the set of other compatible properties which are being measured along with them.

Another notion imposed on classical objects is macrorealism, which is based on two criteria: (i) the object remains in one or the other of many possible states at all times, and (ii) the measurements are *noninvasive*, i.e., they reveal the state of the object without disturbing the object or its future dynamics. Quantum systems are incompatible with these criteria and therefore violate bounds on correlations derived from them. For instance, the Leggett-Garg inequality (LGI) sets up macrorealistic bounds on linear combinations of two-time correlations of a dichotomic observable belonging to a single dynamical system [5]. In this sense, the LGI is regarded as a temporal analog of Bell's inequality. Quantum systems do not comply with the LGI, and therefore provide an important way to distinguish the quantum behavior from macrorealism. Violations of the LGI by quantum systems have been investigated and demonstrated experimentally in various systems [6–17]. Such studies are important in characterizing quantum processors or quantum sensors, where in one would like to know the useful lifetime of a open quantum system gradually decohering towards a classical state [11].

For understanding the quantum behavior it is important to investigate it through different approaches, particularly from an information theoretical point of view. For example, an entropic formulation for Bell's inequality has been given by Braunstein and Caves [18], and later that for contextuality has been given independently by Chaves and Fritz [19] and Kurzyński *et al*. [20]. Recently Usha Devi *et al*. [21] have introduced an entropic formulation of the LGI in terms of classical Shannon entropies associated with classical correlations.

Here we report an experimental demonstration of the violation of the entropic LGI (ELGI) in an ensemble of spin-1/2 nuclei using nuclear magnetic resonance (NMR) techniques. Although NMR experiments are carried out at a high temperature limit, the nuclear spins have long coherence times, and their unitary evolutions can be controlled in a precise way. The large parallel computations carried out in an NMR spin ensemble assists in efficiently extracting the single-event probabilities and joint probabilities. The simplest ELGI study involves three sets of two-time joint measurements of a dynamic observable belonging to a "system" qubit at time instants (t_1,t_2), (t_2,t_3), and (t_1,t_3). The first measurement in each case must be "noninvasive" in the sense that it should not influence the outcome of the second measurement. These noninvasive measurements can be performed with the help of an "ancilla" qubit.

Further, it has been argued in Ref. [21] that the violation of the ELGI arises essentially due to the fact that the joint probabilities do not originate from a legitimate grand probability (of which the joint probabilities are the marginals). Here we also describe extracting the three-time joint probability (grand probability) using a three-qubit system, and demonstrate experimentally that it can not reproduce all the marginal probabilities substantiating this feature.

The paper is organized as follows. In Sec. II we briefly revisit the theory of the ELGI [21], and then we describe the scheme for the measurement of probabilities in Sec. III. Later we detail the experimental study in Sec. IV and describe the study of the three-time joint probability in Sec. V. We conclude in Sec. VI.

*mahesh.ts@iiserpune.ac.in

II. THEORY

Consider a dynamical observable $Q_k := Q(t_k)$ measured at different time instances t_k. Let the measurement outcomes be q_k with probabilities $P(q_k)$. In classical information theory, the amount of information stored in the observable Q_k is given by the Shannon entropy [22], $H(Q_k) = -\sum_{q_k} P(q_k)\log_2 P(q_k)$. Assuming that the observable Q_k has an outcome q_k, the conditional information stored in Q_{k+l} at time t_{k+l} is $H(Q_{k+l}|Q_k = q_k) = -\sum_{q_{k+l}} P(q_{k+l}|q_k)\log_2 P(q_{k+l}|q_k)$, where $P(q_{k+l}|q_k)$ is the conditional probability. Then the mean conditional entropy is given by $H(Q_{k+l}|Q_k) = -\sum_{q_k} P(q_k)H(Q_{k+l}|Q_k = q_k)$. Using Bayes' theorem, $P(q_{k+l}|q_k)P(q_k) = P(q_{k+l},q_k)$, the mean conditional entropy becomes

$$H(Q_{k+l}|Q_k) = H(Q_k,Q_{k+l}) - H(Q_k), \qquad (1)$$

where the joint Shannon entropy $H(Q_k,Q_{k+l}) = -\sum_{q_k,q_{k+l}} P(q_{k+l},q_k)\log_2 P(q_{k+l},q_k)$. These Shannon entropies always follow the inequality [18]

$$H(Q_{k+l}|Q_k) \leqslant H(Q_{k+l}) \leqslant H(Q_k,Q_{k+l}). \qquad (2)$$

The left side of the inequality implies that removing a constraint never decreases the entropy, and the right side implies information stored in two variables is always greater than or equal to that in one [21]. Suppose that three measurements Q_k, Q_{k+l}, and Q_{k+m}, are performed at time instants $t_k < t_{k+l} < t_{k+m}$. Then, from Eqs. (1) and (2), the following inequality can be obtained:

$$H(Q_{k+m}|Q_k) \leqslant H(Q_{k+m}|Q_{k+l}) + H(Q_{k+l}|Q_k). \qquad (3)$$

For n measurements $Q_1, Q_2, \ldots, Q_n$, at time instants $t_1 < t_2 < \cdots < t_n$, the above inequality can be generalized to [21]

$$\sum_{k=2}^{n} H(Q_k|Q_{k-1}) - H(Q_n|Q_1) \geqslant 0. \qquad (4)$$

This inequality must be obeyed by all macrorealistic objects, and its satisfaction means the existence of a legitimate joint probability distribution, which can yield all marginal probabilities [20].

Usha Devi *et al.* [21] have shown theoretically that the above inequality is violated by a quantum spin-s system, prepared in a completely mixed initial state, $\rho_{in} = \mathbb{1}/(2s+1)$. Consider a dynamical observable $Q_t = U_t S_z U_t^\dagger$, with $U_t = e^{i\omega S_x t}$ representing the precession about $\hat{x}$ axis with frequency ω. Let n measurements occur at regular time instants $0, \Delta t, 2\Delta t, \ldots, (n-1)\Delta t$. Ideally in this case, the conditional entropies $H(Q_k|Q_{k-1})$ between successive measurements are all equal, and can be denoted as $H[\theta/(n-1)]$, where $\theta/(n-1) = \omega\Delta t$ is the rotation in the interval Δt. Similarly we can denote $H(Q_n|Q_1)$ as $H[\theta]$. The left-hand side of inequality (4) scaled in units of $\log_2(2s+1)$ is termed as the information deficit $\mathcal{D}$. For n-equidistant measurements, it can be written as [21]

$$\mathcal{D}_n(\theta) = \frac{(n-1)H[\theta/(n-1)] - H[\theta]}{\log_2(2s+1)} \geqslant 0. \qquad (5)$$

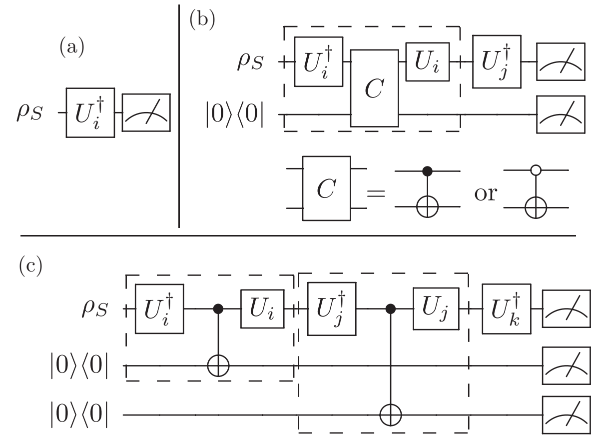

FIG. 1. Circuits for measuring (a) single-event probabilities, (b) two-time joint probabilities, and (c) three-time joint probabilities. The gates grouped by dashed lines represent measurements in the $\{\Pi_0^t,\Pi_1^t\}$ basis. The pointer at the end in each circuit represents the measurement of diagonal elements of the density matrix.

III. MEASUREMENT OF PROBABILITIES

A spin-1/2 particle provides a simple two-level quantum system. Using the eigenvectors $\{|0\rangle,|1\rangle\}$ of S_z, as the computational basis, the projection operators at time $t = 0$ are $\{\Pi_\alpha = |\alpha\rangle\langle\alpha|\}_{\alpha=0,1}$. For the dynamical observable, the measurement basis is rotating under the unitary $U_t = e^{i\omega S_x t}$, such that $\Pi_\alpha^t = U_t \Pi_\alpha U_t^\dagger$. However, it is convenient to perform the actual measurements in the time-independent computational basis. Since for an instantaneous state $\rho(t)$, $\Pi_\alpha^t \rho(t) \Pi_\alpha^t = U_t \Pi_\alpha [U_t^\dagger \rho(t) U_t] \Pi_\alpha U_t^\dagger$, measuring in the $\{\Pi_\alpha^t\}$ basis is equivalent to back evolving the state by $U_t^\dagger$, measuring in the computational basis, and lastly forward evolving by U_t. In the case of multiple-time measurements, the forward evolution can be omitted after the final measurement, since we are interested only in the probabilities and not in the postmeasurement state of the system.

The method for extracting single-event probabilities and joint probabilities involves the quantum circuits shown in Fig. 1. To measure single-event probabilities $P(q_i)$ of a system qubit in a general state ρ_S, it is evolved by $U_i^\dagger = e^{-i\omega S_x t_i}$, and the probabilities $P(q_i)$ are obtained by measuring the diagonal elements of $U_i^\dagger \rho_S U_i$ [Fig. 1(a)].

To measure joint probabilities $P(q_i,q_j)$, we utilize an ancilla qubit initialized in the state $|0\rangle\langle 0|$ [Fig. 1(b)]. After back evolution to the computational basis by $U_i^\dagger$, the CNOT gate encodes the probabilities of the system qubit $P(q_i)$ onto the ancilla qubit. Consider a system qubit initially prepared in a general state ρ_S and an ancilla qubit prepared in the state $|0\rangle\langle 0|$. The CNOT gate encodes the probability of the outcomes in the diagonal elements of the ancilla qubit since

$$\begin{bmatrix} P(0_i) & a \\ a^\dagger & P(1_i) \end{bmatrix}_S \otimes \begin{bmatrix} 1 & 0 \\ 0 & 0 \end{bmatrix}_A \xrightarrow{\text{CNOT}} \begin{bmatrix} P(0_i) & 0 & 0 & a \\ 0 & 0 & 0 & 0 \\ 0 & 0 & 0 & 0 \\ a^\dagger & 0 & 0 & P(1_i) \end{bmatrix}_{SA},$$

where a is the off-diagonal element of the system density matrix. The probabilities $P(0_i)$ and $P(1_i)$ can now be retrieved by tracing over the system qubit and reading the diagonal elements of the ancilla state. After a further evolution by $U_i U_j^\dagger = e^{-i\omega S_x(t_j - t_i)}$, the measurement of diagonal elements of the full two-qubit density matrix yields $P(q_i, q_j)$.

A similar scheme, shown in Fig. 1(c), is employed for extracting the three-time joint probabilities. These circuits can be generalized for higher order joint probabilities or for spin numbers greater than 1/2, using appropriate ancilla register.

In the earlier LGI experiments, noninvasive measurements have been performed by either (i) a weak measurement which causes minimum disturbance to the quantum state [6,9,10] or (ii) initializing the system qubit in a maximally mixed state so that the system density matrix remains unchanged by the measurements [11,12]. Recently however, it was noted by Knee *et al.* that a skeptical macrorealist is not convinced by either of the above methods [23]. Instead, they had proposed a different procedure, viz., an "ideal negative result measurement" (INRM) procedure that is more convincingly noninvasive [17]. The idea is as follows. The CNOT gate is able to flip the ancilla qubit only if the system qubit is in state $|1\rangle$, and does nothing if the system qubit is in state $|0\rangle$ [Fig. 1(b)]. Therefore after the CNOT gate, if we measure the probability of the unflipped ancilla, this corresponds to an "interaction-free" or "noninvasive measurement" of $P(q = 0)$. Similarly, we can implement an anti-CNOT gate, which flips the ancilla only if the system qubit is in state $|0\rangle$, and does nothing otherwise, such that the probability of the unflipped qubit now gives $P(q = 1)$. Note that in both the cases, the probabilities of states wherein the system interacted with the ancilla, resulting in its flip, are discarded. The final measurement need not be noninvasive since we are not concerned about any further evolution.

In our experiments we combine the two methods, i.e., (a) first we prepare the system in a maximally mixed state, i.e., $\rho_S = \mathbb{1}/2$, and (b) we perform an INRM. Theoretically, $P(0_i) = P(1_i) = 1/2$, and the joint probabilities are

$$\begin{aligned} P(0_i, 0_j) &= |\cos(\theta_{ij}/2)|^2/2 = P(1_i, 1_j), \quad \text{and,} \\ P(0_i, 1_j) &= |\sin(\theta_{ij}/2)|^2/2 = P(1_i, 0_j), \end{aligned} \tag{6}$$

where $\theta_{ij} = \omega(t_j - t_i)$ [21].

The only single event entropy needed for the ELGI test is $H(Q_1)$, since $H(Q_1) = H(Q_2)$ for the maximally mixed system state. Further, since $H(Q_1, Q_2) = H(Q_2, Q_3)$ in the case of uniform time intervals, only two joint entropies $H(Q_1, Q_2)$ and $H(Q_1, Q_3)$ are needed to be measured for evaluating $\mathcal{D}_3$. In the following we describe the experimental implementation of these circuits for the three-measurement LGI test.

IV. EXPERIMENT

We have used $^{13}CHCl_3$ (dissolved in $CDCl_3$) as the two qubit system and treat its ^{13}C and ^{1}H nuclear spins as the system and the ancilla qubits, respectively. The J coupling and the molecule are shown in Figs. 2(a) and 2(b). The resonance offset of ^{13}C was set to 100 Hz (provides a dynamic "observable") and that of ^{1}H to 0 Hz (on-resonant). The spin-lattice T_1 and spin-spin T_2 relaxation time constants for

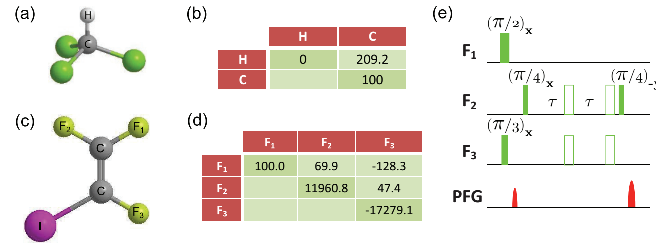

FIG. 2. (Color online) The molecular structures of (a) chloroform and (c) trifluoroiodoethylene and the (b), (d) corresponding tables of relative resonance frequencies (diagonal elements, in Hz) and the J-coupling constants (in Hz). The pulse sequence for initializing trifluoroiodoethylene is shown in (e). In (e) the open pulses are π pulses and the delay $\tau = 1/(4J_{23})$. Pulsed field gradient (PFG) pulses are used to destroy the transverse magnetization.

the ^{1}H spin are, respectively, 4.1 and 4.0 s. The corresponding time constants for ^{13}C are, respectively, 5.5 and 0.8 s. The experiments were carried out at an ambient temperature of 300 K on a 500 MHz Bruker UltraShield NMR spectrometer.

The initialization involved preparing the maximally mixed state $\rho_S = \mathbb{1}/2$ on the system qubit (^{13}C). This is achieved by a $\pi/2$ pulse on ^{13}C followed by a strong pulsed field gradient (PFG). The evolution propagator $U_j^\dagger U_i = e^{-iS_x\omega(t_j - t_i)}$ is realized by the cascade $\mathbb{H} U_d \mathbb{H}$, where $\mathbb{H}$ is the Hadamard gate, and the delay propagator $U_d = e^{-iS_z\omega(t_j - t_i)}$ corresponds to the $\hat{z}$ precession of the system qubit at $\omega = 2\pi 100$ rad/s resonance offset. The J evolution during this delay is refocused by a π pulse on the ancilla qubit. The CNOT, $\mathbb{H}$, as well as the π pulses are realized by numerically optimized amplitude and phase modulated RF pulses, and were robust against the RF inhomogeneity with an average Hilbert-Schmidt fidelity better than 0.998 [24–26]. The final measurement of probabilities are carried out by diagonal tomography. It involved dephasing all the coherences using a strong pulsed field gradient followed by a $\pi/30$ detection pulse. The intensities of the resulting spectral lines yielded a traceless diagonal deviation matrix $\{d_{ii}\}$. The experimental deviation density matrix is normalized with respect to the theoretical traceless density matrix such that they both have the same root mean square value $\sqrt{\sum_i d_{ii}^2}$, and a trace is introduced by adding the identity matrix to the normalized deviation matrix. The resulting diagonal density matrix yields the probabilities.

As described in Fig. 1(b), two sets of experiments were performed, one with CNOT and the other with anti-CNOT. We extracted $P(0,q)$ $(q = \{0,1\})$ from the CNOT set, and $P(1,q)$ from the anti-CNOT set. The probabilities thus obtained by the INRM procedure are plotted in Fig. 3. These sets of experiments also allow us to compare the results from (i) only CNOT, (ii) only anti-CNOT, and (iii) INRM procedures. The joint entropies were calculated in each case using the experimental probabilities and the information deficit (in bits) was calculated using the expression $\mathcal{D}_3 = 2H(Q_2|Q_1) - H(Q_3|Q_1)$. The theoretical and experimental values of $\mathcal{D}_3$ for various rotation angles θ are shown in Fig. 4. We find a general agreement between the mean experimental $\mathcal{D}_3$ values with that of the quantum theory. The error bars indicate the standard deviations obtained by a series of independent measurements. According

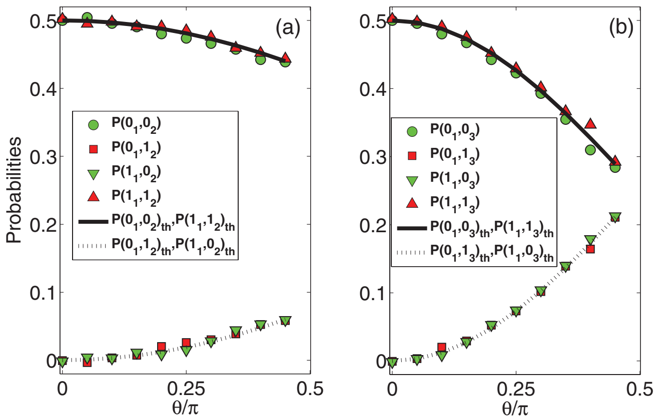

FIG. 3. (Color online) The lines indicate the theoretical joint probabilities (a) $P(q_1,q_2)_{\text{th}}$ and (b) $P(q_1,q_3)_{\text{th}}$, and the symbols indicate the mean experimental probabilities (a) $P(q_1,q_2)$ and (b) $P(q_1,q_3)$ obtained by the INRM procedure.

to quantum theory, a maximum violation of $\mathcal{D}_3 = -0.134$ should occur at $\theta = \pi/4$. The experimental values of $\mathcal{D}_3(\pi/4)$ are -0.141 ± 0.005 [Fig. 4(a)], -0.136 ± 0.002 [Fig. 4(b)], and -0.114 ± 0.027 [Fig. 4(c)] for the CNOT, anti-CNOT, and INRM cases, respectively. Thus in all the cases, we found a clear violation of ELGI.

V. THREE-TIME JOINT PROBABILITY

In the above, we have described extracting the two-time joint probabilities $P(q_i,q_j)$ directly. However, it should also be possible to generate them as marginals $P'(q_i,q_j)$ of three-time joint probabilities:

$$P'(q_1,q_2) = \sum_{q_3} P(q_1,q_2,q_3),$$
$$P'(q_2,q_3) = \sum_{q_1} P(q_1,q_2,q_3), \quad \text{and} \qquad (7)$$
$$P'(q_1,q_3) = \sum_{q_2} P(q_1,q_2,q_3).$$

In a macrorealistic world $P'(q_i,q_j) = P(q_i,q_j)$.

The above equality can be investigated experimentally by measuring the three-time joint probabilities, as described in Fig. 1(c). Since this experiment requires measurements at three time instants, we need two ancilla qubits along with the system qubit. We use the three ^{19}F nuclear spins (each spin 1/2) of trifluoroiodoethylene dissolved in acetone-D6 as the three-qubit system [Figs. 2(c) and 2(d)]. Here the first spin F_1 is used as the system qubit and the others, F_2 and F_3, are chosen as the ancilla qubits. The effective ^{19}F transverse relaxation time constants T_2^* were about 0.8 s and their longitudinal relaxation time constants were all longer than 6.3 s. The experiments were carried out at an ambient temperature of 290 K. The initialization involved evolution of an equilibrium deviation density matrix under the sequence shown in Fig. 2(e):

$$\begin{gathered} S_{1z} + S_{2z} + S_{3z} \\ \downarrow (\pi/2)_{1x}(\pi/3)_{3x}, \text{PFG} \\ S_z^2 + \frac{1}{2}S_{3z} \\ \downarrow (\pi/4)_{2x} \\ \frac{1}{\sqrt{2}}S_{2z} - \frac{1}{\sqrt{2}}S_{2y} + \frac{1}{2}S_{3z} \\ \downarrow 1/(2J_{23}) \\ \frac{1}{\sqrt{2}}S_{2z} + \sqrt{2}S_{2x}S_{3z} + \frac{1}{2}S_{3z} \\ \downarrow (\pi/4)_{-2y}, \text{PFG} \\ \frac{1}{2}(S_{2z} + 2S_{2z}S_{3z} + S_{3z}). \end{gathered}$$

The above deviation density matrix is equivalent to the traceless part of $\frac{1-\epsilon}{8}\mathbb{1} + \epsilon\{\frac{1}{2}\mathbb{1}_S \otimes |00\rangle\langle 00|_A\}$ where $\epsilon \sim 10^{-5}$ is the purity factor [27].

First we obtained the three-time joint probabilities $P(q_1,q_2,q_3)$ using the circuit in Fig. 1(c). Two-time marginal probabilities $P'(q_i,q_j)$ were obtained using Eqs. (7). Note that the circuits measuring higher order joint probabilities can also be used to retrieve lower order joint probabilities by selectively tracing out qubits. Therefore, two-time joint probabilities $P(q_i,q_j)$ were measured directly with the same circuit [Fig. 1(c)]; here the joint probabilities are completely stored in the ancilla qubits, and were obtained by tracing out the system qubit. The experimental results of $P(q_1,q_2)$ and $P'(q_1,q_2)$ are shown in Fig. 5(a). It is evident that the marginals agree quite well with the corresponding joint probabilities. Similarly experimental results of $P(q_1,q_3)$ and $P'(q_1,q_3)$ are shown in Fig. 5(b). However, here we see significant deviation of marginal probabilities from joint probabilities.

These results show, in contrary to the macrorealistic theory, that the grand probability $P(q_1,q_2,q_3)$ can not reproduce all

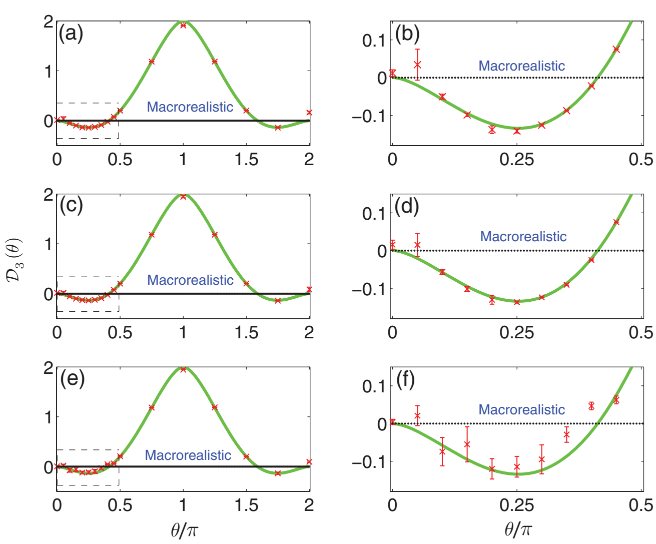

FIG. 4. (Color online) Information deficit $\mathcal{D}_3$ versus θ obtained with (a), (b) CNOT; (c), (d) anti-CNOT; and (e), (f) INRM procedure. The boxed areas in the left plots [(a), (c), (e)] are magnified in the right plots [(b), (d), (f)], respectively. The mean experimental $\mathcal{D}_3$ (in bits) values are shown as symbols. The curves indicate theoretical $\mathcal{D}_3$ (in bits). The horizontal lines at $\mathcal{D}_3 = 0$ indicate the lower bounds of the macrorealism territories.

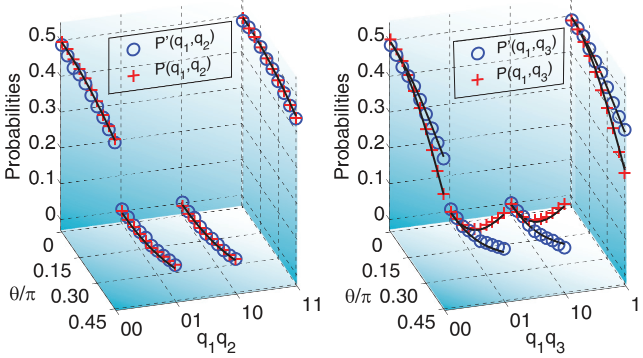

FIG. 5. (Color online) (a) Joint probabilities $P(q_1,q_2)$ and marginal probabilities $P'(q_1,q_2)$, and (b) joint probabilities $P(q_1,q_3)$ and marginal probabilities $P'(q_1,q_3)$. The lines correspond to theoretical values and the symbols are mean experimental values.

the two-time joint probabilities as the marginals. Therefore the grand probability is not legitimate in the quantum case, which is the fundamental reason for the violation of the ELGI by quantum systems [21].

It is interesting to note that even for those values of θ for which $\mathcal{D}_3$ is positive, the three-time joint probability is illegitimate. Therefore, while the violation of the ELGI indicates the quantumness of the system, its satisfaction does not rule out the quantumness.

VI. CONCLUSIONS

We described an experimental study of the entropic Leggett-Garg inequality in nuclear spins using NMR techniques. We employed the recently described ideal negative result measurement procedure to noninvasively extract joint probabilities. Our results indicate the macrorealistic bound being violated by over four standard deviations, confirming the nonmacrorealistic nature of the spin-$1/2$ particles. Further, we have experimentally measured the three-time joint probabilities and confirmed that the two-time joint probabilities are not reproduced as the marginals. Thus, quantum systems do not have legitimate joint probability distribution, which results in the violation of bounds set-up for macrorealistic systems.

One distinct feature of the entropic LGI is that the dichotomic nature of observables assumed in the original formulation of the LGI can be relaxed, thus allowing one to study the quantum behavior of higher dimensional systems, such as those with spin numbers greater than $1/2$. This could be an interesting topic for future experimental investigations.

ACKNOWLEDGMENTS

The authors are grateful to Prof. Usha Devi, Prof. A. K. Rajagopal, Dr. G. C. Knee, Prof. Anil Kumar, Dr. V. Athalye, and Dr. S. S. Roy for discussions. This work was partly supported by the DST Project SR/S2/LOP-0017/2009.

[1] A. Einstein, B. Podolsky, and N. Rosen, Phys. Rev. **47**, 777 (1935).
[2] J. Bell, Physics **1**, 195 (1964).
[3] S. Kochen and E. P. Specker, J. Math. Mech. **17**, 59 (1967).
[4] J. S. Bell, Rev. Mod. Phys. **38**, 447 (1966).
[5] A. J. Leggett and A. Garg, Phys. Rev. Lett. **54**, 857 (1985).
[6] A. Palacios-Laloy *et al.*, Nat. Phys. **6**, 442 (2010).
[7] N. Lambert, R. Johansson, and F. Nori, Phys. Rev. B **84**, 245421 (2011).
[8] J.-S. Xu, C.-F. Li, X.-B. Zou, and G.-C. Guo, Sci. Rep. **1**, 101 (2011).
[9] M. E. Goggina *et al.*, Proc. Natl. Acad. Sci. USA **108**, 1256 (2011).
[10] J. Dressel, C. J. Broadbent, J. C. Howell, and A. N. Jordan, Phys. Rev. Lett. **106**, 040402 (2011).
[11] V. Athalye, S. S. Roy, and T. S. Mahesh, Phys. Rev. Lett. **107**, 130402 (2011).
[12] A. M. Souza, I. S. Oliveira, and R. S. Sarthour, New J. Phys. **13**, 053023 (2011).
[13] C. Emary, Phys. Rev. B **86**, 085418 (2012).
[14] Y. Suzuki, M. Iinuma, and H. F. Hofmann, New J. Phys. **14**, 103022 (2012).
[15] S. Yong-Nan *et al.*, Chin. Phys. Lett. **29**, 120302 (2012).
[16] Z.-Q. Zhou, S. F. Huelga, C.-F. Li, and G.-C. Guo, arXiv:1209.2176 [quant-ph].
[17] G. C. Knee *et al.*, Nat. Commun. **3**, 606 (2012).
[18] S. L. Braunstein and C. M. Caves, Phys. Rev. Lett. **61**, 662 (1988).
[19] R. Chaves and T. Fritz, Phys. Rev. A **85**, 032113 (2012).
[20] P. Kurzyński, R. Ramanathan, and D. Kaszlikowski, Phys. Rev. Lett. **109**, 020404 (2012).
[21] A. R. Usha Devi, H. S. Karthik, Sudha, and A. K. Rajagopal, Phys. Rev. A **87**, 052103 (2013).
[22] M. A. Nielsen and I. L. Chuang, *Quantum Computation and Quantum Information* (Cambridge University Press, Cambridge, 2000).
[23] G. C. Knee, E. M. Gauger, G. A. D. Briggs, and S. C. Benjamin, New J. Phys. **14**, 058001 (2012).
[24] E. M. Fortunato *et al.*, J. Chem. Phys. **116**, 7599 (2002).
[25] T. S. Mahesh and D. Suter, Phys. Rev. A **74**, 062312 (2006).
[26] N. Khaneja *et al.*, J. Magn. Reson. **172**, 296 (2005).
[27] D. G. Cory, M. D. Price, and T. F. Havel, Physica D **120**, 82 (1998).